BIOCELL
2023 47(7): 1595-1609

Tech Science Press

Bushen Yizhi Formula regulates the IRE1α pathway to alleviate endoplasmic reticulum stress in an Alzheimer's disease rat model

Xiru XU[1,#]; Yuan FANG[1,#]; Biao ZHANG[1,*]; Shichao TENG[1]; Xiang WU[1]; Jing ZHANG[1]; Xiaoqun GU[2]; Meixia MA[3]

[1] Geriatrics Department, Affiliated Hospital of Nanjing University of Chinese Medicine, Nanjing, China
[2] School of Pharmacy, Nanjing University of Chinese Medicine, Nanjing, China
[3] The First Clinical Medical College, Nanjing University of Chinese Medicine, Nanjing, China

Key words: Bushen Yizhi Formula, Alzheimer's disease, Endoplasmic reticulum stress, IRE1α

Abstract: Background: While the Bushen Yizhi Formula can treat Alzheimer's disease (AD), the yet to be ascertained specific mechanism of action was explored in this work. **Methods:** Different concentrations of the Bushen Yizhi Formula and amyloid-beta peptide (Aβ) were used to treat rat pheochromocytoma cells (P12) and human neuroblastoma cells (SH-SY5Y). Cell morphological changes were observed to determine the *in vitro* cell damage. Cell Counting Kit (CCK)-8 assay and flow cytometry were employed to identify cell viability and apoptosis/cell cycle, respectively. Western blotting and immunohistochemistry were employed to measure the expressions of endoplasmic reticulum stress (ERS)-related proteins (GRP78 and CHOP), p-IRE1α, IRE1α, ASK1, p-JNK, JNK, Bax, Bcl-2, XBP-1, and Bim. Fura 2-acetoxymethyl ester (Fura-2/AM) was used to determine the intracellular calcium (Ca^{2+}) concentration. Also, an AD model was constructed by injecting Aβ into the CA1 area of the hippocampus in Sprague Dawley rats. AD model rats were gavaged with different concentrations of Bushen Yizhi Formula for 14 consecutive days. The Morris water maze experiment was conducted to test the learning and memory of rats. Hematoxylin & Eosin (H&E) and Terminal-deoxynucleotidyl Transferase (TdT)-mediated dUTP Nick-End Labeling (TUNEL) staining were done to determine histopathological changes in the brain. **Results:** Bushen Yizhi Formula relieved the Aβ-induced effects including cell injury, decreased viability, increased apoptosis, G0/G1 phase cell cycle arrest, up-regulation of GRP78, CHOP, p-IRE1α, p-JNK, Bax, XBP-1 and Bim, as well as down-regulation of Bcl-2. These results were also seen with IRE1α silencing. While Aβ suppressed the learning and memory abilities of rats, the Bushen Yizhi Formula alleviated these effects of Aβ. Brain nerve cell injury induced by Aβ could also be treated with Bushen Yizhi Formula. **Conclusion:** Bushen Yizhi Formula could influence ERS through the IRE1α signaling pathway to achieve its therapeutic effects on AD.

Introduction

Neurodegenerative diseases are unique neurological diseases affecting the survival and function of neurons in the brain (Davis *et al.*, 2018; Tracy and Gan, 2018; Shi *et al.*, 2020). Loss of neurons often leads to a decline in cognitive function, which could induce dementia (Shi *et al.*, 2020). According to the World Health Organization (WHO), the number of people with dementia globally reached 47.47 million in 2015. This figure could reach 75.63 million by 2030 and even 135.46 million by 2050 (Shi *et al.*, 2020). Alzheimer's disease (AD) is the most common cause of neurodegenerative diseases (Mckhann *et al.*, 2011). With the increase in the aged society, we have to pay great attention to AD (Alzheimer's Association, 2016). AD is characterized by pathological misfolding and aggregation of amyloid-beta peptide (Aβ) and hyperphosphorylated tau. Aβ is a major component of amyloid plaques, the extracellular deposits found in the brains of people with AD. Plaques form when certain types of Aβ, such as Aβ38/40/42, aggregate together in sufficient quantities to form small clumps of protein that gradually accumulate (Tiwari *et al.*, 2019). Extensive Aβ plaque deposition in the cortex is the most significant pathological marker of AD (Sadleir *et al.*, 2018). In recent years, a variety of therapeutic drugs for AD have been assessed clinically (Wong *et al.*, 2019).

*Address correspondence to: Biao Zhang, zhangbiao1969@njucm.edu.cn
#These authors contributed equally to this work
Received: 10 November 2022; Accepted: 16 January 2023;
Published: 23 June 2023

Doi: 10.32604/biocell.2023.027697

However, as these drugs did not have a significant therapeutic effect, searching for a new drug for AD is of great significance.

The Bushen Yizhi Formula is mostly used in Chinese medicine to treat dementia. It is an effective combination of herbs for the treatment of AD derived from the theory of traditional Chinese medicine (Zhang *et al.*, 2017a). The Bushen Yizhi Formula consists of the following components: *Fructus Cnidii*, *Panax ginseng*, *Polygonum multiflorum*, *Cortex moutan*, *Ligustrum lucidum*, and *Fructus lycii* (Cai *et al.*, 2018). Current studies have proved that Bushen Yizhi Formula has a therapeutic effect on AD (Zhang *et al.*, 2017b). Notably, Bushen Yizhi Formula ameliorates cognition deficits and attenuates oxidative stress-related neuronal apoptosis in scopolamine-induced senescence in mice (Hou *et al.*, 2014). Further, Bushen Yizhi Formula exerts anti-AD effects by alleviating scopolamine (SCOP)-induced cognitive impairment (Zhang *et al.*, 2017a), and ameliorating cognitive dysfunction through the sirtuin 1 (SIRT1)/endoplasmic reticulum stress (ERS) pathway in aging mice (Zhang *et al.*, 2017b). However, as the specific mechanism of action is not yet clear, Bushen Yizhi Formula cannot be widely used globally at present.

A growing body of evidence indicates that ERS may be the main mechanism for the development of AD (Hedskog *et al.*, 2013; Hashimoto and Saido, 2018). In view of this, we speculated that Bushen Yizhi Formula may treat AD through the intervention of ERS. Studies showed that ERS triggered the unfolded protein response (UPR), and prolonged ER stress-related perturbations. This might enhance the UPR-induced cytotoxicity to thereby induce apoptosis (Fu and Gao, 2014; Gardner *et al.*, 2013; Yasmeen *et al.*, 2022). Inositol-requiring enzyme 1 (IRE1) is one of the three transmembrane receptor proteins in the ER. It contains kinase and ribonuclease domains in the cytoplasm (Hillary and Fitzgerald, 2018). In cells experiencing ERS, IRE1 undergoes autophosphorylation and activates endoribonuclease activity (Chen and Brandizzi, 2013). The mammalian IRE1 gene encodes two subtypes: IRE1α and IRE1β (Feldman *et al.*, 2019). Ongoing research on human diseases is focused more on IRE1α. This is because IRE1α has been proven to be involved in the development and progression of AD by a large amount of evidence (Duran-Aniotz *et al.*, 2017; Montibeller and de Belleroche, 2018; Sadleir *et al.*, 2018). In light of the above data, this study was aimed at authenticating whether Bushen Yizhi Formula affects ERS through the IRE1α signaling pathway to treat AD.

To probe the *in vitro* and *in vivo* therapeutic effects of Bushen Yizhi Formula on AD, the present study first constructed *in vitro* and *in vivo* models of AD using Aβ-treated cells and rats, respectively. In addition, we also assessed the specific mechanism of Bushen Yizhi Formula in the treatment of AD, to provide a certain theoretical basis for the treatment of AD by Bushen Yizhi Formula. As there are multiple mechanisms for Traditional Chinese Medicine treatment in AD therapy, further regulatory mechanisms and clinical trials of Bushen Yizhi Formula still need to be further investigated.

Materials and Methods

Ethical statement

All animal experiments were conducted in accordance with the guidelines of the China Council on Animal Care and Use. All experiments involving animals were conducted at the Zhejiang Laboratory Animal Center and approved in advance by the Institutional Animal Care and Use Committee of Zhejiang Laboratory Animal Center (Approval No. ZJCLA-IACUC-20040024).

Establishment of the Alzheimer's disease rat model and treatment

In this study, 36 Sprague Dawley rats (male and female, 250–280 g, 8 months old) were selected as experimental subjects. All rats were purchased from Beijing Weitong Lihua Laboratory Animal Technology Co., Ltd. (Beijing, China, https://www.vitalriver.com/). All the rats were housed in a specific pathogen-free room under standard conditions (humidity: 50–60%, temperature: 22–25°C; 12-hour (h)/12-h day/night cycle) with free access to food and water for the duration of the study. The establishment process of the AD rat model is discussed as follows: rats were anesthetized by an intraperitoneal injection (40 mg/kg) of 1% pentobarbital sodium. In the rats, the anterior fontanelle of the skull was 4.4 mm backward, 2.2 mm paralateral and 3.0 mm subdural. 10 μg of Aβ was slowly injected into the hippocampus by a microinjection pump. The needle was kept for 5 minutes (min), and the same dose of Aβ was injected into the contralateral hippocampus. Rats in the sham operation group were injected with normal saline in the same way. After injection, the wound of the rats was sutured and the operative area was disinfected. The water maze learning and memory test were conducted 7 days after the model establishment.

Rats were divided into 6 groups (6 rats/group) and treated as follows: Normal group (rats with Sham operation were gavaged with normal saline for 14 consecutive days); Aβ group (AD model rats were gavaged with normal saline for 14 consecutive days); BSYZ-L+Aβ group (AD model rats were gavaged with a low concentration of Bushen Yizhi Formula [1.46 g/kg/d] for 14 consecutive days); BSYZ-M +Aβ group (AD model rats were gavaged with a medium concentration of Bushen Yizhi Formula [2.92 g/Kg/d] for 14 consecutive days); BSYZ-H+Aβ group (AD model rats were gavaged with a high concentration of Bushen Yizhi Formula [5.84 g/Kg/d] for 14 consecutive days); and BSYZ-H group (rats with sham operation group were gavaged with a high concentration of Bushen Yizhi Formula for 14 consecutive days) (Zhang, 2017).

To obtain the treated sera for cell experiments, after 4 days of treatment with each concentration of Bushen Yizhi Formula, sera were collected 1 h after the last treatment. The sera from rats in each group were added to the medium at 10% concentration as the cell culture medium.

Cell culture, treatment and morphological analysis

Rat pheochromocytoma cells (PC12) and human neuroblastoma cells (SH-SY5Y) were selected as the subjects

of the cell experiment in this study. Both types of cells were routinely cultured in low glucose DMEM/F12 medium (11330032, Gibco, Grand Island, NY, USA) containing 10% fetal bovine serum (10099-141, Gibco) and 1% penicillin-streptomycin antibiotics (15070063, Gibco). Cells were cultured in an incubator containing 5% CO_2 at 37°C.

The PC12 and SH-SY5Y cells were divided into 8 groups according to the experimental design and treated as follows: Normal group (PC12 or SH-SY5Y cells were cultured with normal medium), PBS+Aβ group (PC12 or SH-SY5Y cells were treated with PBS and incubated with 5 μmol/L Aβ [HY-P1388/HY-P1363, Medchemexpress, Danvers, MA, USA]), BSYZ-L+Aβ group (PC12 or SH-SY5Y cells were treated with the low concentration of Bushen Yizhi Formula treated sera for 24 h and then incubated with 5 μmol/L Aβ), BSYZ-M+Aβ group (PC12 or SH-SY5Y cells were treated with the medium concentration of Bushen Yizhi Formula treated sera for 24 h and then incubated with 5 μmol/L Aβ), BSYZ-H+Aβ group (PC12 or SH-SY5Y cells were treated with the high concentration of Bushen Yizhi Formula treated sera for 24 h and then cultivated with 5 μmol/L Aβ), Vector+Aβ group (PC12 or SH-SY5Y cells were transfected with the empty vector for 24 h and then incubated with 5 μmol/L Aβ), ShIRE1α+Aβ group (PC12 or SH-SY5Y cells were transfected with short hairpin RNA [shIRE1α] for 24 h and then cultivated with 5 μmol/L Aβ), and IRE1α+Aβ group (PC12 or SH-SY5Y cells were transfected with an IRE1α overexpression plasmid for 24 h and then continued to be incubated with 5 μmol/L Aβ).

The treated PC12 or SH-SY5Y cells were placed under an inverted microscope (magnification: 100×; Olympus Corporation, Tokyo, Japan) to observe their morphological changes.

Cell transfection assays

The shIRE1α (5′-CCGGATGGAGCTGAGGGCACAATTG CTCGAGCAATTGTGCCCTCAGCTCCATTTTTTG-3′) and the IRE1α overexpression plasmid used for transfection were constructed by GenePharm (Shanghai, China). Transfection procedures listed in the instructions (11668-027, Invitrogen, Carlsbad, CA, USA) provided by the transfection reagent supplier were followed. Briefly, PC12 and SH-SY5Y cells were placed in a 6-well plate at a density of 2×10^5 cells per well. The culture medium of cells was changed to serum-free medium after 18 h, and the transfection was conducted after culture for another 6 h. Plasmids and Lipofectamine 2000 were diluted with 250 μL Opti-MEM, respectively. After incubating for 5 min, the plasmid diluent and Lipofectamine 2000 diluent were mixed. The mixture was incubated for another 20 min and then added to the corresponding cells. The culture medium containing the transfection reagent was replaced with the normal medium after 6 h. The transfection efficiency of the plasmids was detected by quantitative reverse transcription polymerase chain reaction (qRT-PCR) and Western blotting after 24 h or 48 h.

Cell counting kit-8 assay

PC12 and SH-SY5Y cells were seeded in 96-well plates at a density of 3000 cells per well. The proliferation of PC12 and SH-SY5Y cells was detected by the CCK-8 reagent (C0038, Beyotime) after the various treatments described above. Here, 10 μL of the CCK-8 reagent was added to the cells at 24, 36, and 72 h, respectively. The cells were cultured in an incubator for another 3 h, and the optical density (OD) value at 450 nm was then measured with a microplate reader (Molecular Devices, Sunnyvale, CA, USA). All experiments were performed in triplicate.

Flow cytometry

Flow cytometry was used to detect the condition of cell apoptosis as follows: after the cells were treated according to the above groups, trypsin without Ethylene Diamine Tetraacetic Acid (EDTA, 15090046, Gibco) was used to digest the cells for 2 min. Then, 1 mL of medium was added to the cells for terminating digestion, and the cells were then transferred to a 1.5 mL centrifuge tube. Subsequently, the cells were centrifuged in a 125×g centrifuge (4°C) for 5 min. The culture medium was removed, and the cells were resuspended with precooled phosphate buffer saline (PBS). The cells were again centrifuged in a 125×g centrifuge (4°C) for 5 min. Then, the cell washing step in PBS was repeated twice. After removal of PBS, the cells were resuspended with 100 μL of 1 × Binding Buffer (556547, Becton, Dickinson and Company, Franklin Lakes, NJ, USA), followed by the addition of 5 μL Propidium Iodide (PI) and Fluorescein 5-isothiocyanate (FITC). Thereafter, the dyes were mixed and incubated at room temperature for 15 min in the dark. Subsequently, 400 μL of 1 × Binding buffer was used to re-suspend the cells, and the cells were gently combined into a single cell. Finally, a flow cytometer (Becton, Dickinson, and Company) was used to study cell apoptosis. All experiments were performed in triplicate.

The cell cycle analysis was done by flow cytometry as follows: cells were firstly washed with PBS and then immobilized with pre-cooled 70% alcohol for 4 h. Subsequently, the cells were washed again with PBS, followed by being immersed in 500 μL of PI staining solution (C1052, Beyotime). Later, the cell cycle was analyzed by a flow cytometer after the cells were incubated at room temperature for 30 min in the dark. All experiments were performed in triplicate.

Detection of calcium concentration

After the treatment of the cells as mentioned above, the culture medium was removed and the cells were washed three times with HEPES Buffered Saline (HBS, C0218, Beyotime), with each time for 5 min. Then, the cells were incubated with 2.5 μM of Fura-2/AM at 37°C for 30 min in the dark. After incubation, the culture medium was removed and the cells were washed three times with HBS (5 min for each time). The cells were then incubated in an incubator for 30 min. Cells were alternatively excited with light from a xenon lamp passed through a high-speed monochromator at 340/380 nm. All experiments were performed in triplicate.

Morris water maze experiment

The device used in this experiment was a round pool with a diameter of 160 cm and a height of 50 cm (Shanghai XinRuan Information Technology Co., Ltd., Shanghai,

China, http://www.softmaze.com/s02/article/2012/06/19/621828.html). The pool was filled with water (temperature: 23 ± 2°C) dyed black to a depth of 30 cm. Four equidistant points (N, E, S, and W) were marked on the pool wall as the starting point of the experiment and the pool was divided into four quadrants. The central placing platform of the SW area was selected. After the end of the intervention experiment, the rats were subjected to Morris water maze behavior detection for 7 days. The positioning navigation experiment was performed on the 1st to 6th day, and the space exploration experiment was carried out on the 7th day. The training was conducted on the 1st to 2nd day, and fixed-time training was conducted daily in the morning and afternoon (more than 2 h apart). The time required for the rats to find the platform (escape from the incubation period) was recorded. Likewise, the circuit diagram and total distance of the rats were recorded. If the rats could not find the platform within 90 seconds (s), they were guided to the platform and put back into the cage after staying on the platform for 15 s, and the escape incubation period of the rats was recorded as 90 s. On the 3rd to 6th day, the rats were placed into the pool from the opposite side quadrant and the adjacent quadrant at a fixed time, and the escape incubation period and the first arrival time in the SW area were recorded twice a day. On day 7, the platform was removed and the rats were placed into the pool from the contralateral quadrant. The number of times the rats crossed the original platform position, and the swimming time in the quadrant where the platform was located in 90 s were recorded.

Histological analyses

Rats were intraperitoneally injected with 3% pentobarbital sodium (0.3 mL) after the Morris water maze experiment. After successful anesthesia administration, the chest was cut open and the right auricular part was also cut open. Cardiac perfusion was performed first with 100 mL normal saline, and then slowly with 250 mL of 4% paraformaldehyde (P0099, Beyotime) at 4°C for 24 h. After that, the rat brain tissue samples were removed and paraffin-embedded. Then, the tissue was sliced, dewaxed, and rehydrated. Briefly, paraffin-embedded rat brain tissue was cut into 5 μm sections and then dewaxed with xylene twice (10 min for each time). The sections were then rehydrated in gradient alcohol (100%, 90%, 80%, and 70%) for 5 min.

For hematoxylin-eosin (H&E staining), the above sections were dyed in hematoxylin dyeing solution (C0105, Beyotime) for 5 min, followed by being differentiated with hydrochloric acid ethanol for 30 s. After being placed in eosin solution for 3 min of staining, the sections were routinely dehydrated by gradient alcohol, made transparent using xylene, and sealed with neutral resin. Finally, the sections were observed and photographed by an inverted microscope.

For Terminal-deoxynucleotidyl Transferase (TdT)-mediated dUTP Nick-End Labeling (TUNEL) staining, protease K (50 μL) working solution was added to the above sections at 37°C for 30 min. Then, 3% H_2O_2 was added to the tissue samples, and incubated at room temperature for 20 min. Afterward, the sections were treated with 50 μL of biotin-labeled solution (C1091, Beyotime) at 37°C for 60 min of incubation in the dark, followed by further incubation with 100 μL of labeled termination solution at room temperature for 10 min. Subsequently, 50 μL of streptavidin-HRP working solution was added to the sections, and then 3, 3′-diaminobenzidine (DAB) staining was performed for 5 min. After routine dehydration, the samples were made transparent and sealed. Finally, an inverted microscope was employed for observing and photographing.

For immunohistochemistry: the above sections were treated with 1% goat serum (C0265, Beyotime) and incubated at room temperature for 1 h, followed by being treated with primary antibody solution (GRP78, ab21685, 1:1000, rabbit, Abcam, Cambridge, MA, USA; CHOP, SAB5700602, 1:100, Sigma, St. Louis, MO, USA) at 4°C for overnight incubation. After being washed three times with PBS, the sections were incubated with the secondary antibody (ab6721, 1:10000, Abcam) at room temperature for 1 h. This was followed by DAB staining, routine dehydration after which tissues were made transparent by xylene treatment finally sealed. Ultimately, the sections were placed under an inverted microscope for observing and photographing.

Western blotting

The cells or tissues were lysed in ice-cold RIPA buffer (P0013B, Beyotime) containing 1% protease inhibitor (P1030, Beyotime) and 2% phosphatase inhibitor (P1081, Beyotime) for 15 min. The samples were then centrifuged at 10,000 rpm for 10 min at 4°C. Equal amounts of samples (30 μg) and 4 μL of Marker (PR1910, Solarbio, Beijing, China) were separated on a sodium dodecyl sulfate-polyacrylamide gel electrophoresis (SDS-PAGE) gel. Then, the samples were placed onto PVDF membranes (ISEQ00010/IPVH00010, Millipore, MA, USA), followed by being blocked with 5% skim milk at room temperature for 1 h. Afterward, the membranes were incubated with primary antibodies against the following proteins: Inositol-Requiring enzyme 1α (IRE1α; ab37073, 107 kDa, 1:1000, Rabbit, Abcam), phosphorylated (p)-IRE1α (ab124945, 110 kDa, 1:1000, Rabbit, Abcam), Apoptosis Signal Regulating Kinase 1 (ASK1; ab45178, 155 kDa, 1:1000, Rabbit, Abcam), c-Jun N-Terminal Kinase (JNK; ab179461, 54/46 kDa, 1:1000, Rabbit, Abcam), p-JNK (ab124956, 54/46 kDa, 1:5000, Rabbit, Abcam), BCL2-Associated X (Bax; ab32503, 21 kDa, 1:5000, Rabbit, Abcam), B-Cell Lymphoma 2 (Bcl-2; ab59348, 26 kDa, 1:1000, Rabbit, Abcam), X-Box Binding Protein 1 (XBP1; ab37152, 29 kDa, 1:2000, Rabbit, Abcam), Bcl-2 interacting mediator of cell death (Bim; ab32158, 22 kDa, 1:2000, Rabbit, Abcam), Glucose-Regulated Protein (GRP78; ab21685, 75 kDa, 1:1000, Rabbit, Abcam), C/EBP-Homologous Protein (CHOP; ab11419, 31kDa, 1:5000, mouse, Abcam), and Glyceraldehyde-3-Phosphate Dehydrogenase (GAPDH; ab8245, 36 kDa, 1:5000, mouse, Abcam) overnight at 4°C. The next day, the membranes were treated with HRP-conjugated secondary antibodies (ab6789, 1:5000, Abcam; ab6721, 1:10000, Abcam) at room

temperature for 1 h. Finally, the protein band was visualized by ECL solution (NEL105001EA, PerkinElmer, PerkinElmer Inc., Waltham, MA, USA) and specific Image Analysis Software (Version 2.2.1, PerkinElmer Inc., Waltham, MA, USA). GAPDH served as an internal reference. All experiments were performed in triplicate.

Statistical analysis

SPSS 20.0 (IBM, NY, USA) was used for statistical analysis. All data were expressed as mean ± standard deviation (SD). One-way ANOVA analysis of variance was used for comparison between groups, followed by the Tukey post-hoc tests. A difference of $p < 0.05$ was deemed to be statistically significant.

Results

Bushen Yizhi Formula and Inositol-requiring enzyme 1α (IRE1α) silencing reduced the amyloid-beta peptide (Aβ)-induced morphological damage and decreased cell viability

As the changes in cell morphology reflect the state of the cells, we first observed the morphology of cells in each treatment group under a microscope. Compared with the normal group cells, Aβ-treated PC12, and SH-SY5Y cells exhibited significant morphological damage (Figs. 1A and 1B). Interestingly, Bushen Yizhi Formula (BSYZ-F) alleviated the effects of Aβ in a concentration-dependent manner (Figs. 1A and 1B). In addition, while IRE1α silencing also alleviated the effects of Aβ, overexpression of IRE1α potentiated the effects of Aβ (Figs. 1A and 1B). Subsequently, the results of the CCK-8 assay also showed that PC12 and SH-SY5Y cells exposed to Aβ treatment documented reduced viability, as compared with the normal group cells (Figs. 1C and 1D, $p < 0.01$). Similarly, Bushen Yizhi Formula and IRE1α silencing alleviated the effects of Aβ (Figs. 1C and 1D, $p < 0.05$, $p < 0.01$). On the contrary, overexpression of IRE1α promoted the effects of Aβ.

Bushen Yizhi Formula and IRE1α silencing decreased apoptosis and G0/G1 phase cell arrest induced by Aβ

In order to assay the effects of Bushen Yizhi Formula and IRE1α on cell apoptosis, we used flow cytometry to detect the apoptosis of cells in each group. As can be seen in Figs. 2A and 2B, Aβ-treated cells documented increased apoptosis relative to the normal group cells ($p < 0.001$). Furthermore, BSYZ-F and shIRE1α partially alleviated the Aβ-induced apoptosis, and the effect of BSYZ-F was seen in a concentration-dependent manner (Figs. 2A and 2B, Suppl. Fig. 1, $p < 0.01$, $p < 0.001$). Besides, we also found that IRE1α overexpression promoted the apoptosis induced by Aβ (Figs. 2A and 2B, Suppl. Fig. 1, $p < 0.001$). Further tests showed that Bushen Yizhi Formula alleviated the Aβ-induced G0/G1 phase cell cycle arrest in a concentration-dependent manner, and this effect was also shown by shIRE1α treatment (Figs. 2C and 2D, Suppl. Fig. 2, $p < 0.05$, $p < 0.01$). On the contrary, up-regulation of IRE1α further promoted the G0/G1 phase cell cycle arrest induced by Aβ (Figs. 2C and 2D, Suppl. Fig. 2, $p < 0.05$).

Bushen Yizhi Formula and IRE1α silencing reduced levels of GRP78, CHOP and calcium induced by Aβ

Before we began to evaluate the effects of Bushen Yizhi Formula and IRE1α on ERS, we first measured the relationship between Aβ and ERS. As detailed in Figs. 2E and 2F, the expression of GRP78 and CHOP were elevated in Aβ-induced cells compared to those in the normal group cells ($p < 0.001$). We further found that Bushen Yizhi Formula and shIRE1α partially reduced the expression of GRP78 and CHOP, which were enhanced by Aβ, while overexpression of IRE1α further promoted GRP78 and CHOP expression (Figs. 2E and 2F, $p < 0.05$, $p < 0.01$, $p < 0.001$). Additionally, Ca^{2+} concentration was increased in the PBS+Aβ group as compared with that in the normal group (Figs. 2G and 2H, $p < 0.05$). Similarly, while Bushen Yizhi Formula and shIRE1α decreased the concentration of Ca^{2+}, IRE1α overexpression exerted the opposite effects (Figs. 2G and 2H, $p < 0.05$).

Bushen Yizhi Formula blocked the IRE1α signaling pathway activated by Aβ

We also explored the relationship between Bushen Yizhi Formula and the IRE1α signaling pathway. Our test results proved that the expression levels of Bax, XBP-1, and Bim, together with the ratios of p-IRE1α/IRE1α and p-JNK/JNK, were increased, the expression of Bcl-2 was decreased, when compared with those in the normal group cells (Fig. 3, $p < 0.001$). Bushen Yizhi Formula partially reversed these effects of Aβ in a dose-dependent manner (Fig. 3, $p < 0.05$, $p < 0.001$). In addition, IRE1α overexpression enhanced the effects of Aβ, while the results of IRE1α silencing was in contrast (Fig. 3, $p < 0.01$, $p < 0.001$). However, the expression of ASK1 among the groups displayed no significant difference (Fig. 3).

Bushen Yizhi Formula partially improved the learning and memory abilities of the AD rat models

The trajectory of the rat space exploration data revealed that the percentage of time in the quadrant of the platform of the Aβ-treated rats was significantly lower than that of the normal rats (Fig. 4A). The percentage of time of Aβ-treated rats in the quadrant where the platform was located was significantly increased following the treatment with the Bushen Yizhi Formula in a concentration-dependent manner (Fig. 4A). However, the high dose of the Bushen Yizhi Formula did not change the learning and memory abilities of the normal rats (Fig. 4A). The results of the Morris water maze navigation experiment showed that the escape latency time of AD rats was increased compared with normal rats (Fig. 4B, $p < 0.001$). However, compared with AD rats, the escape latency time of AD rats treated with Bushen Yizhi Formula was decreased (Fig. 4B, $p < 0.05$, $p < 0.01$, $p < 0.001$). Compared with normal rats, AD rats took a much longer time to reach the platform the first time (Fig. 4C, $p < 0.001$). Subsequent tests found that the Bushen Yizhi Formula could relatively shorten the time of the first arrival of AD rats at the platform (Fig. 4C, $p < 0.001$). However, the Bushen Yizhi Formula did not completely offset the effects of Aβ (Fig. 4C, $p < 0.05$). Further, the Morris water maze space exploration experiment results showed that AD rats

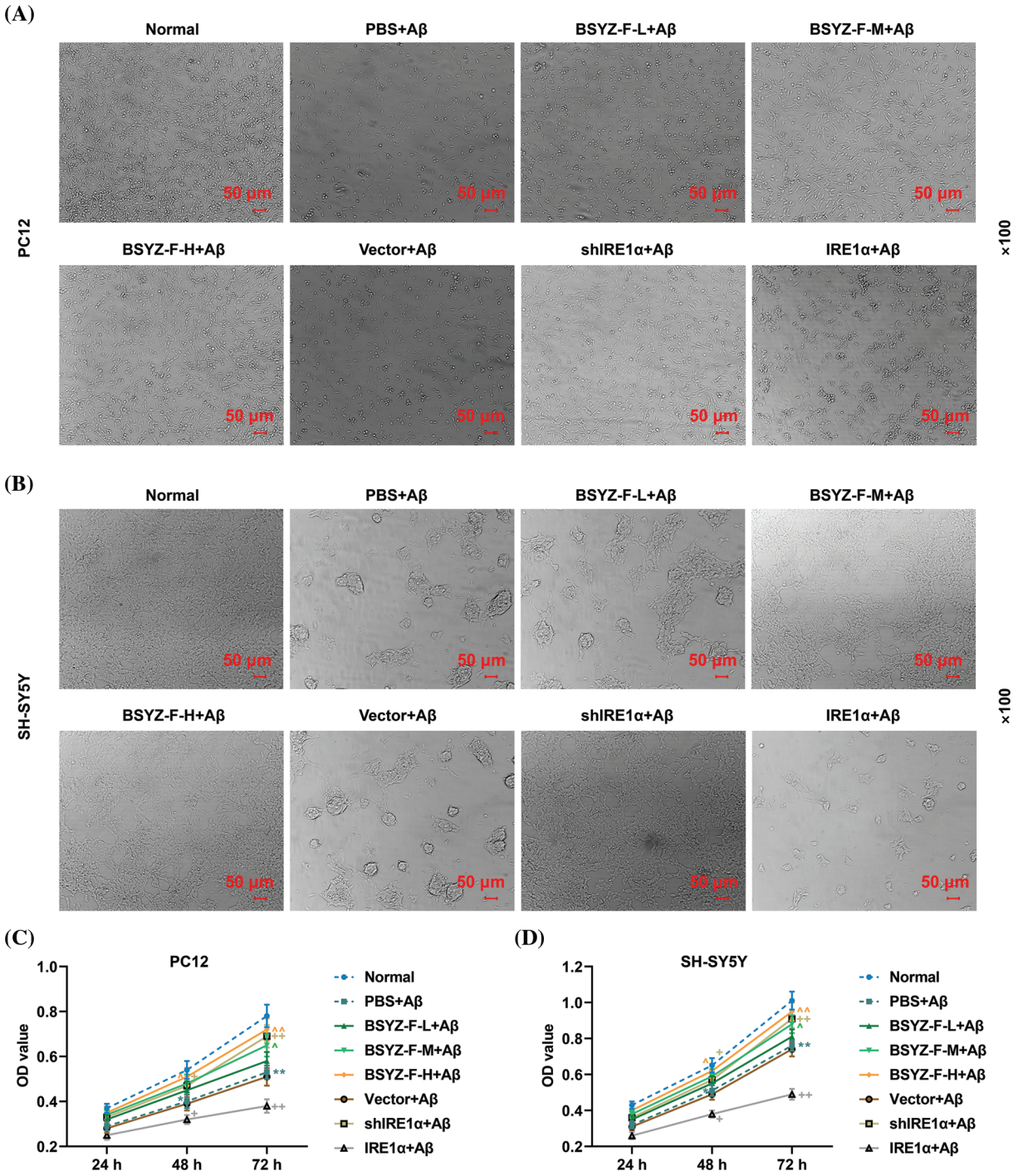

FIGURE 1. Bushen Yizhi Formula and IRE1α silencing reversed Aβ-induced morphological damage and decreased cell viability. (A, B) Cell morphology of PC12 and SH-SY5Y cells was observed by an inverted microscope. (C, D) Cell viability of PC12 and SH-SY5Y cells was detected by CCK-8 assay. * *vs.* Normal, ^ *vs.* PBS+Aβ, + *vs.* Vector+Aβ; ^ or +or * $p < 0.05$, ^^ or ++ or ** $p < 0.01$. IRE1α: Inositol-Requiring enzyme 1α; Aβ: amyloid-beta peptide; CCK-8, cell counting kit-8; BSYZ-F, Bushen Yizhi Formula.

crossed the platform and swam in the quadrant of the platform for a less time duration than normal rats (Figs. 4D and 4E, $p < 0.001$). The Bushen Yizhi Formula could partially alleviate the effects of Aβ on rats, but it could not completely cure the rats (Figs. 4D and 4E, $p < 0.05$, $p < 0.01$, $p < 0.001$).

Bushen Yizhi Formula could alleviate Aβ-induced brain nerve injury in rats

As the most obvious characteristic of AD is the damage to brain nerve cells, we observed the damage to brain nerve cells by H&E and TUNEL staining. The results of the H&E staining showed that in normal rats, the nerve cells in brain tissue were evenly arranged, with abundant cytoplasm and nerve cells, and the extracellular space between cells was normally distributed (Fig. 5A). In contrast, Aβ treatment resulted in structural damage to brain cells, vascular obstruction or necrosis, inflammatory infiltration, and reduced neuronal activity in rats (Fig. 5A). The dose-dependent decrease of edema and necrosis at brain injury sites and the number of nerve cells were effectively

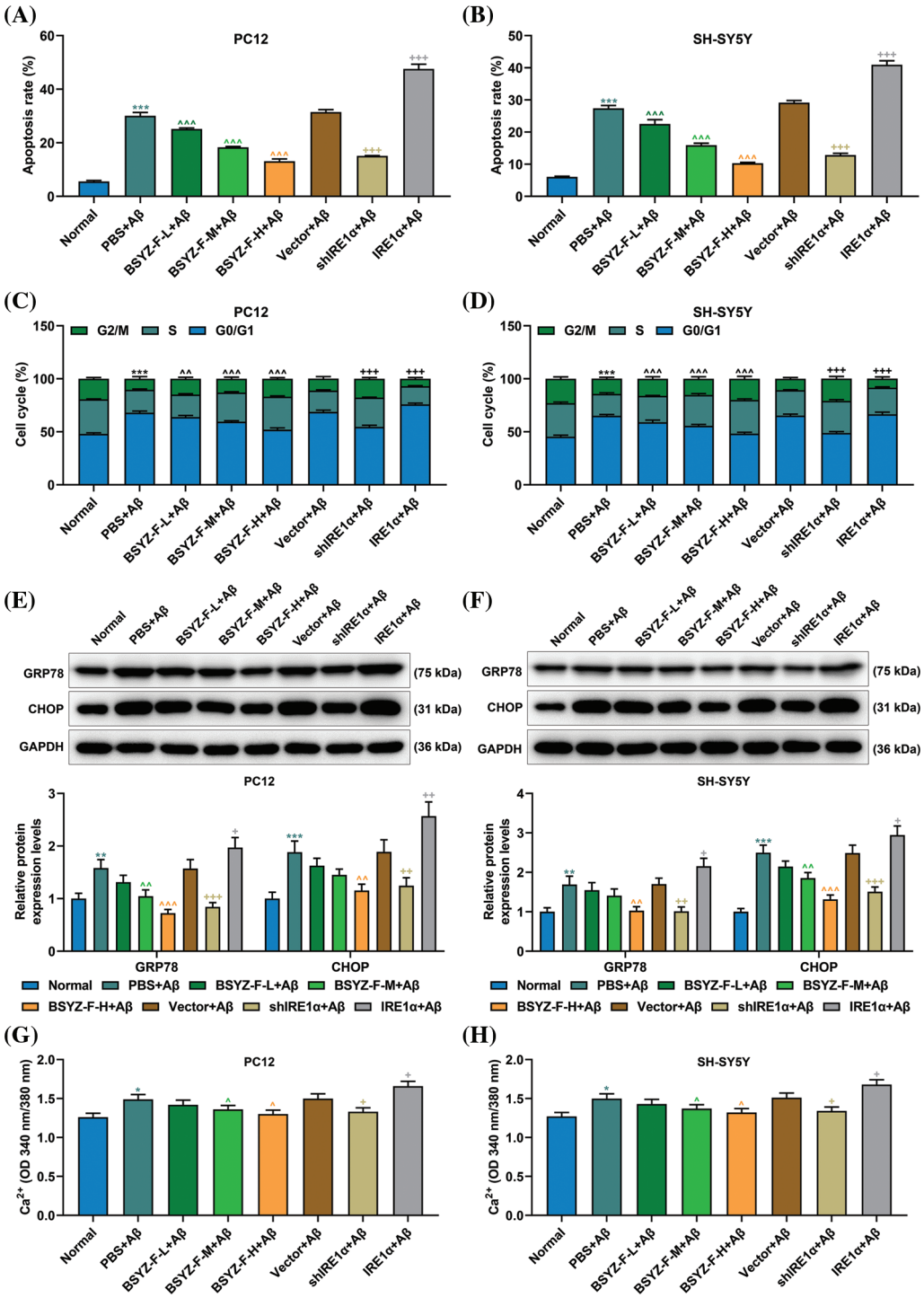

FIGURE 2. Bushen Yizhi Formula and IRE1α silencing reversed Aβ-induced cell apoptosis, G0/G1 cell cycle arrest, GRP78 and CHOP expression and increased calcium contents. (A, B) The apoptosis of PC12 and SH-SY5Y cells was measured by flow cytometry. (C, D) The cell cycle of PC12 and SH-SY5Y cells was assayed by flow cytometry. (E, F) Expressions of GRP78 and CHOP were determined by Western blotting. (G, H) The content of Ca^{2+} was determined by the commercial kit. * *vs.* Normal, ^ *vs.* PBS+Aβ, + *vs.* Vector+Aβ; ^^ $p < 0.01$, ^^^or +++ or *** $p < 0.001$. IRE1α: Inositol-Requiring enzyme 1α; Aβ: amyloid-beta peptide; BSYZ-F: Bushen Yizhi Formula; GRP78: glucose regulated protein 78; CHOP: C/EBP-homologous protein.

increased after the treatment with Bushen Yizhi Formula (Fig. 5A). In addition, TUNEL staining showed apoptosis of the hippocampal dentate gyrus in AD rats, as compared with that in the normal group rats (Figs. 5B and 5C, $p < 0.001$). On the same lines, the Bushen Yizhi Formula reversed the effects of Aβ in a dose-dependent manner but did not completely cure the brain nerve injury in rats (Figs. 5B and 5C, $p < 0.01$, $p < 0.001$).

Bushen Yizhi Formula alleviated ERS induced by Aβ by blocking the IRE1α pathway

In order to further explore the mechanism of nerve injury in AD rat brain tissue, we carried out further assays. The expressions of ERS-related proteins GRP78 and CHOP were first detected by immunohistochemistry and Western blotting. As illustrated by Figs. 5D–5F, Aβ increased the expression levels of GRP78 and CHOP as compared to the

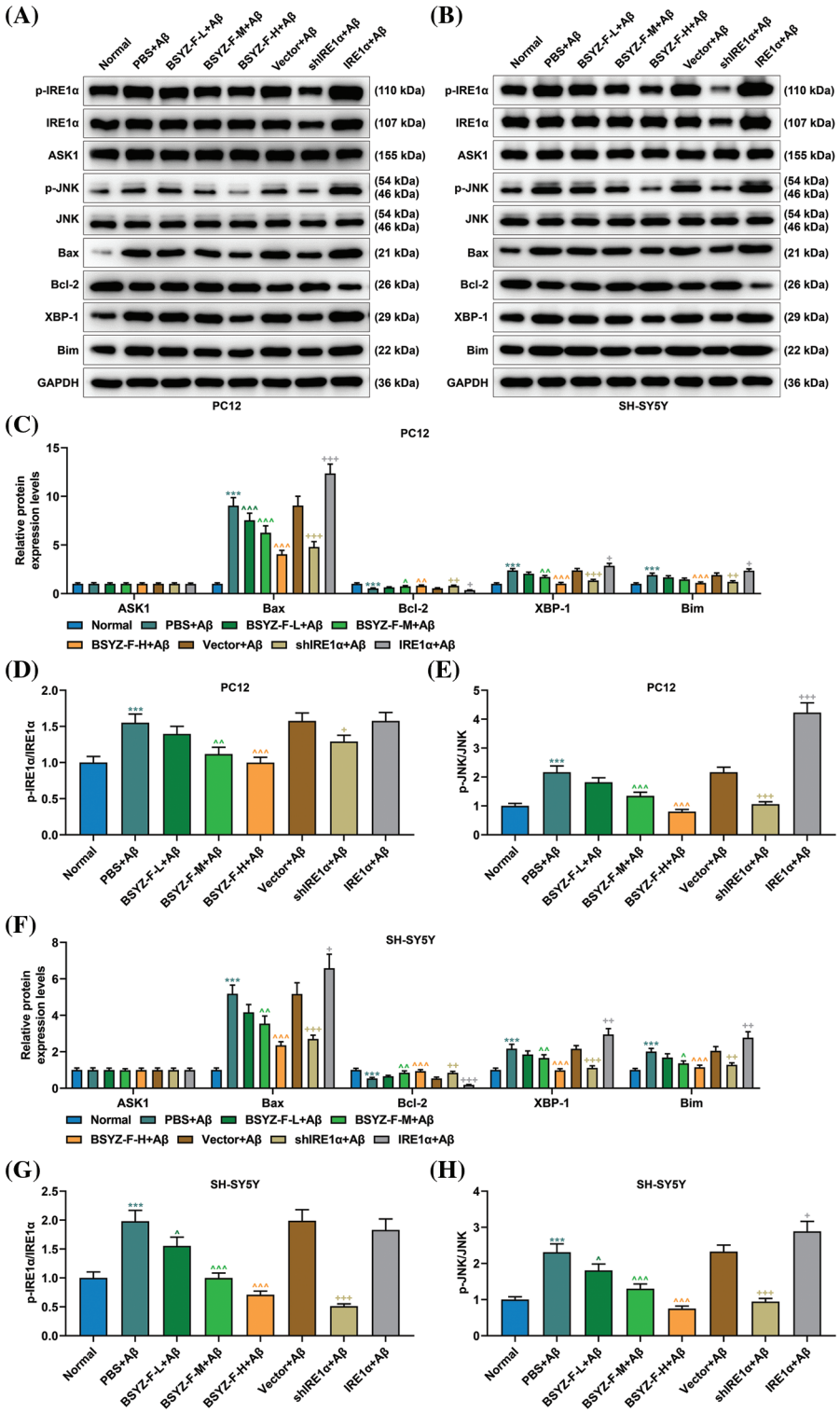

FIGURE 3. Bushen Yizhi Formula alleviated the blocking of the IRE1α signaling pathway caused by Aβ. (A–C, F). Expressions of p-IRE1α, IRE1α, ASK1, p-JNK, JNK, Bax, Bcl-2, XBP-1, and Bim were identified by Western blotting. (D, E, G, H). The ratio of p-IRE1α and IRE1α or p-JNK/JNK was calculated. * *vs.* Normal, ^ *vs.* PBS+Aβ, + *vs.* Vector+Aβ; ^ or + or * $p < 0.05$, ^^ or ++ or ** $p < 0.01$, ^^^or +++ or *** $p < 0.001$. IRE1α: Inositol-Requiring enzyme 1α; Aβ: amyloid-beta peptide; ASK1: apoptosis signal-regulating kinase 1; JNK: c-Jun N-terminal kinase; Bax: Bcl-2 associated X; Bcl-2: B-cell lymphoma-2; XBP-1: X-box binding protein I; Bim: Bcl-2 interacting mediator of cell death; BSYZ-F: Bushen Yizhi Formula.

normal group ($p < 0.001$). The Bushen Yizhi Formula partially alleviated the effect of Aβ (Figs. 5D–5F, $p < 0.05$, $p < 0.01$). Subsequently, the expression of proteins related to the IRE1α signal pathway was then detected. As detailed in Figs. 6A–6E, Aβ promoted the expression of p-IRE1α, p-JNK, Bax, XBP-1, and Bim, the expression of Bcl-2 was inhibited compared with the normal group ($p < 0.001$). The Bushen Yizhi Formula could partly reverse the effect of Aβ

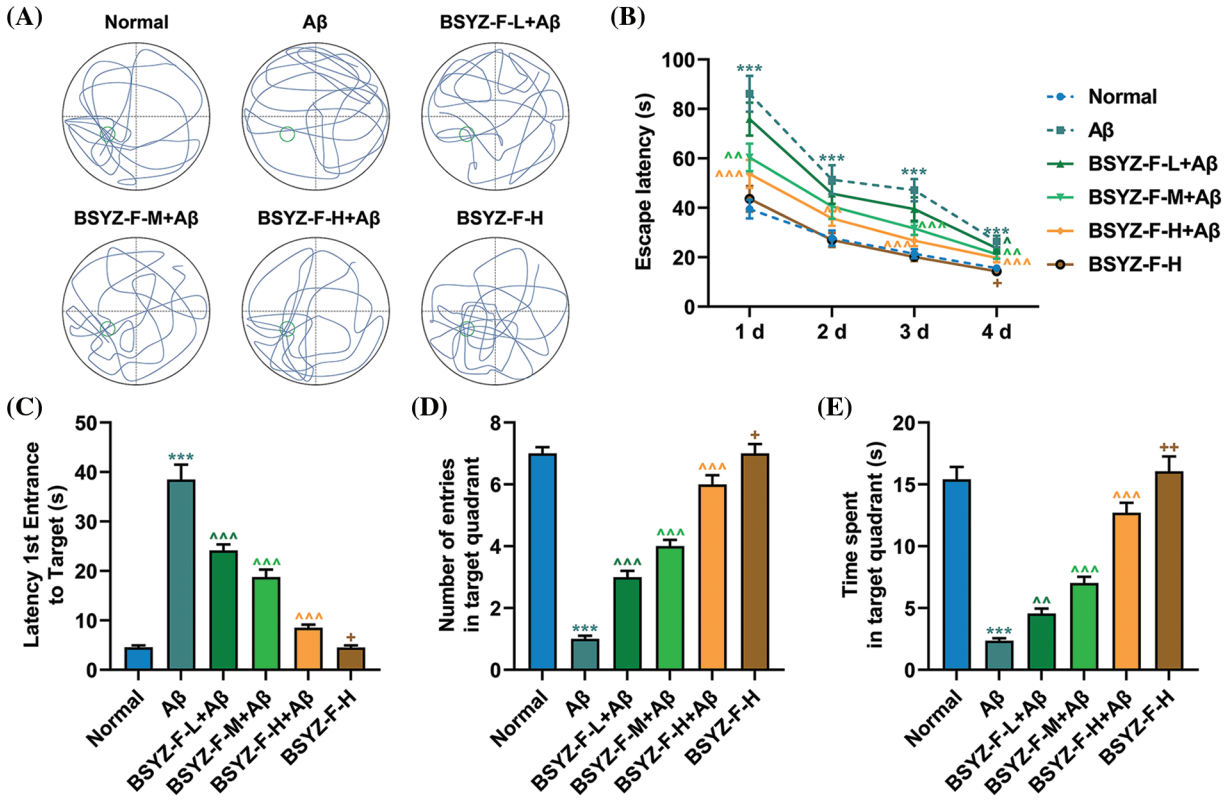

FIGURE 4. Bushen Yizhi Formula reversed the decline of learning and memory abilities in the AD rat model caused by Aβ. (A) The trajectories of rats in the space exploration experiment. (B–E) The escape latency, latency 1st entrance to the target, number of entries in the target quadrant, and time spent in the target quadrant of rats were recorded. * *vs.* Normal, ^ *vs.* Aβ, + *vs.* BSYZ-F-H+Aβ; + $p < 0.05$, ^^ $p < 0.01$, ^^^ or *** $p < 0.001$. Aβ: amyloid-beta peptide; BSYZ-F, Bushen Yizhi Formula.

on p-IRE1α, p-JNK, Bax, XBP-1, Bim, and Bcl-2 expression levels (Figs. 6A–6E, $p < 0.05$, $p < 0.01$, $p < 0.001$).

Discussion

AD is a common neurodegenerative disease worldwide (Tanzi, 2012). In addition to the neuronal loss mentioned earlier, another important pathological feature of AD is the deposition of Aβ in the brain (Sweeney *et al.*, 2018). Therefore, in this study, *in vivo* or *in vitro* models of AD were constructed by treating cells and rats with Aβ, respectively. Based on these, we found that Bushen Yizhi Formula inhibited the ERS through the IRE1α signaling pathway and improved Aβ-induced effects *in vitro* and *in vivo*. These results revealed one of the mechanisms of the Bushen Yizhi Formula on ERS in our AD model and provided experimental evidence that the Bushen Yizhi formula may be a potent preparation to treat AD.

AD is attributed to extracellular aggregates of Aβ plaques and neurofibrillary tangles (Li *et al.*, 2018). PC12 and SH-SY5Y cells were treated with Aβ to establish an *in vitro* AD cell model, and the results showed that Aβ decreased the viability of PC12 and SH-SY5Y cells, induced apoptosis and G0/G1 phase arrest. This was similar to the results by another research team (Liu *et al.*, 2021). Moreover, the Bushen Yizhi Formula alleviated the decreased cell viability and the increased apoptosis induced by Aβ, which was similar to the findings of another report that the Bushen Yizhi Formula improved the viability of $A\beta_{1\text{-}42}$-treated PC12 cells (Zhang *et al.*, 2017a). In our *in vivo* AD model, Aβ induced brain nerve tissue lesions and decreased the learning and memory abilities of rats. These results lead us to believe that our cell (*in vitro*) and rat (*in vivo*) models of AD were successful.

We then tested the therapeutic efficacy of the Bushen Yizhi Formula by treating our AD models. The results verified that the Bushen Yizhi Formula alleviated the brain nerve damage induced by Aβ. Further, the Bushen Yizhi formula also alleviated Aβ-induced memory and learning decline in rats. Based on these results, we believe that by alleviating the neurotoxicity caused by Aβ, the Bushen Yizhi Formula could improve the Aβ-induced damage to the learning and memory abilities in rats. This result is consistent with previous studies (Zhang *et al.*, 2017a, 2017b; Cai *et al.*, 2018). Further, the Bushen Yizhi formula could ameliorate memory impairment in ibotenic acid-induced AD rats by modulating cholinergic pathways and NGF signaling, and preventing apoptosis (Hou *et al.*, 2014). Additionally, the Bushen Yizhi formula treatment could shorten the escape latency, and increase both in time spent in the quadrant of the platform placed and crossing counts in AD model mice (Hou *et al.*, 2014).

The current mainstream research believes that the pathogenesis of AD may be related to ERS (Endres and Reinhardt, 2013; Logue *et al.*, 2013). The ER is the main site of protein synthesis modification, carbohydrate, lipid

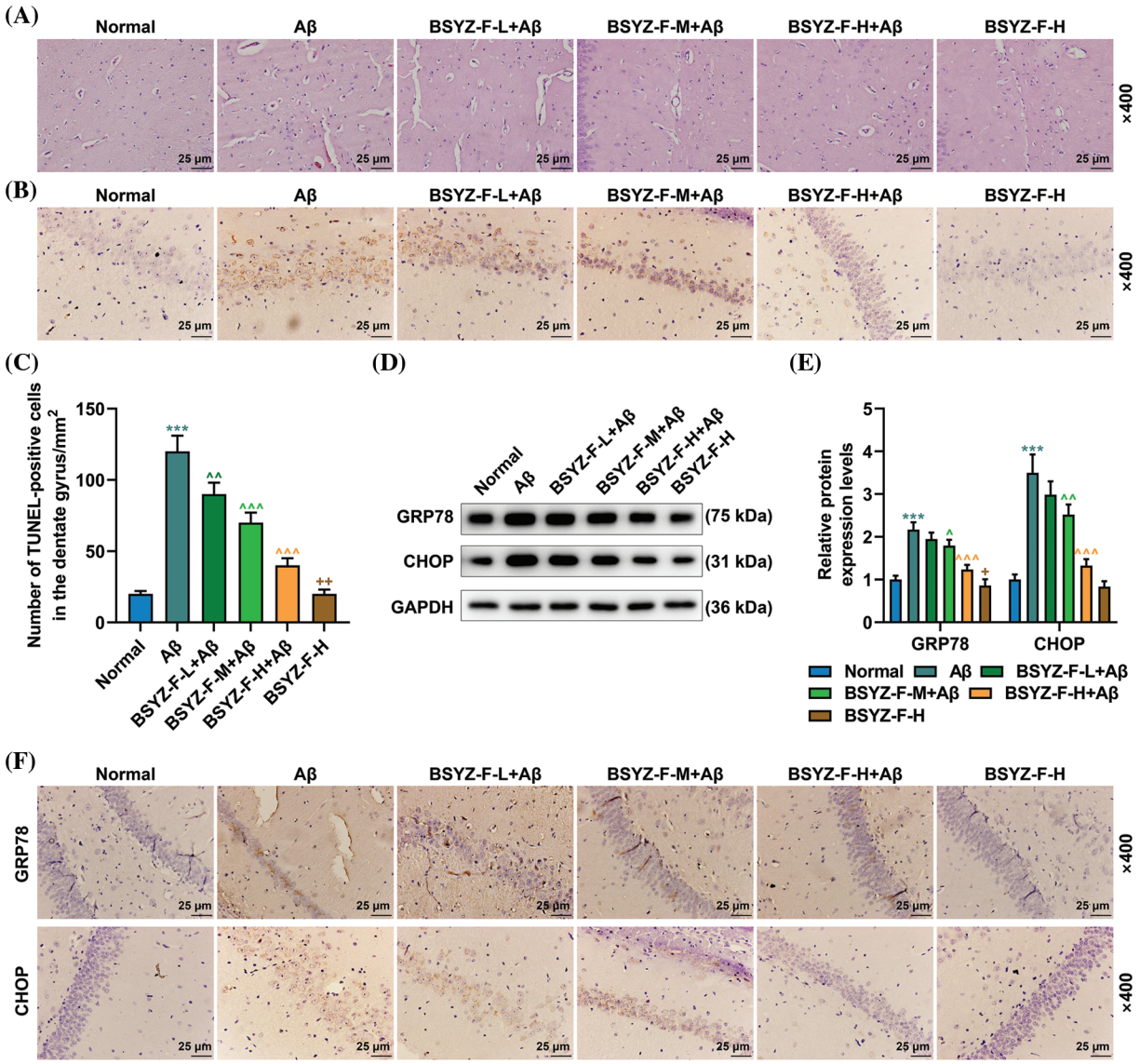

FIGURE 5. Bushen Yizhi Formula alleviated Aβ-induced brain nerve injury in rats. (A) The pathological changes in the rat brain samples were identified by H&E staining. (B, C) TUNEL staining was used to identify the level of neuronal apoptosis in rat brain tissue. (D–F) The expression levels of GRP78 and CHOP were measured by Western blot and immunohistochemistry. * *vs.* Normal, ^ *vs.* Aβ, + *vs.* BSYZ-F-H+Aβ; + $p < 0.05$, ++ or ^^ $p < 0.01$, ^^^ or *** $p < 0.001$. Aβ: amyloid-beta peptide; H&E: hematoxylin-eosin staining; TUNEL: Terminal-deoxynucleoitidyl Transferase Mediated Nick-End Labeling; GRP78: glucose regulated protein 78; CHOP: C/EBP-homologous protein; BSYZ-F: Bushen Yizhi Formula.

synthesis, and Ca^{2+} storage in cells, and its abnormal function could cause a series of pathophysiological changes in cells (Qi and Chen, 2019). The three transmembrane receptor proteins on the endoplasmic reticulum are protein kinase RNA-like endoplasmic reticulum kinase (PERK), activating transcription factor 6 (ATF6), and IRE1, which can sense the stress signal within the endoplasmic reticulum (Song *et al.*, 2018). All these three proteins are in an inactive state by binding to GRP78 in the endoplasmic reticulum lumen under normal conditions (Ibrahim *et al.*, 2019). As the number of misfolded and unfolded proteins in the ER accumulates, GRP78 disengages from these transmembrane receptor proteins that are activated the dissociation from the GRP78 complex (Zhang, 2017). CHOP, also known as growth stagnation and DNA loss gene 153, is responsible for the regulation of apoptosis-related proteins Bcl-2 and Bim genes in the ER (Jung *et al.*, 2015). By detecting the expression changes of these two genes, we found that Aβ increased the expressions of GRP78 and CHOP. This indicated that Aβ induced ERS in PC12, SH-SY5Y cells, and rat brain nerve cells. As expected, the Bushen Yizhi Formula ameliorated the Aβ-induced ERS in a concentration-dependent manner. In addition, the increase in Ca^{2+} content induced by Aβ treatment was also reversed by the Bushen Yizhi Formula. This suggests that the Bushen Yizhi Formula addresses AD by relieving ERS. A previously study also revealed that the Bushen Yizhi Formula decreased CHOP expression and relieved ERS in SAMP8 mice (Zhang *et al.*, 2017b).

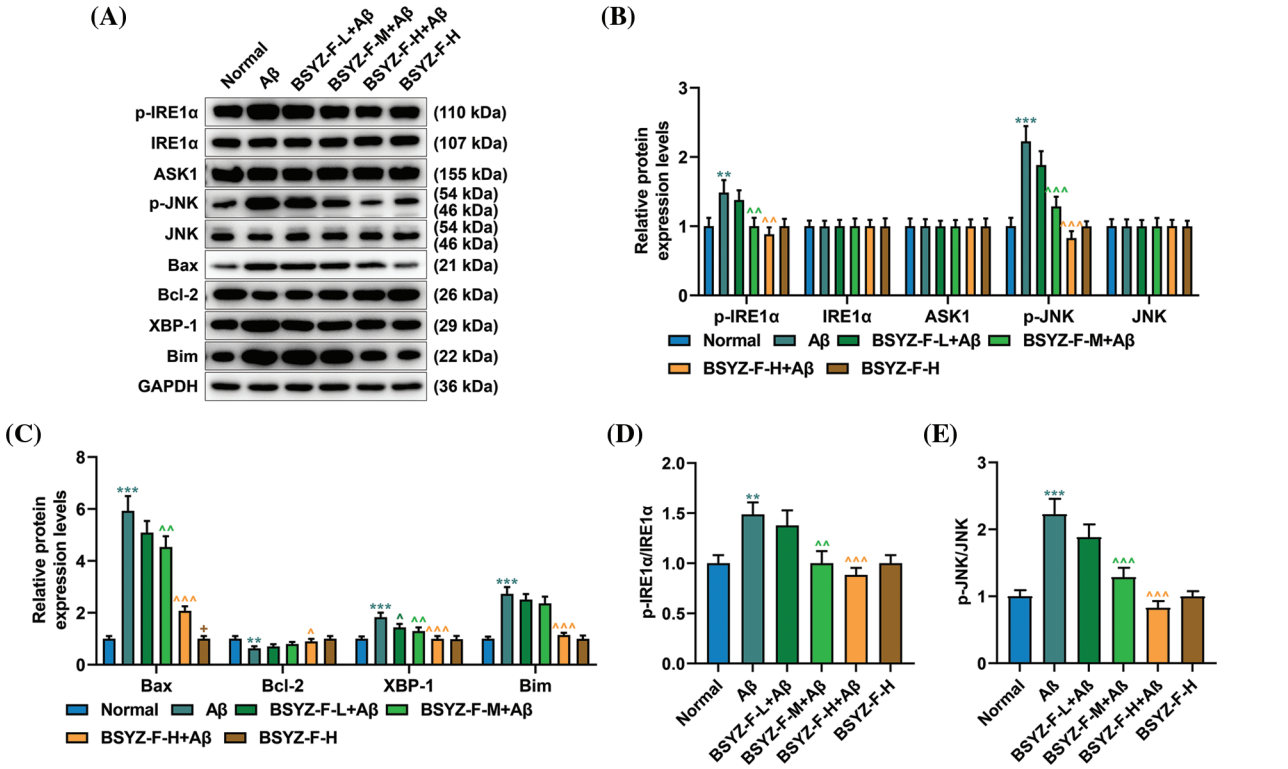

FIGURE 6. Bushen Yizhi Formula alleviated the blocking of the IRE1α signaling pathway caused by Aβ in rats. (A–C) Expressions of p-IRE1α, IRE1α, ASK1, p-JNK, JNK, Bax, Bcl-2, XBP-1, and Bim were quantified by Western blot. (D, E) The ratio of p-IRE1α and IRE1α or p-JNK/JNK was calculated. * *vs.* Normal, ^ *vs.* Aβ, $^{+}$ *vs.* BSYZ-F-H+Aβ; $^{+}$ $p < 0.05$, ^^ $p < 0.01$, ^^^ or *** $p < 0.001$. IRE1α: Inositol-Requiring enzyme 1α; Aβ: amyloid-bata peptide; ASK1: apoptosis signal-regulating kinase 1; JNK: c-Jun N-terminal kinase; Bax: Bcl-2 associated X; Bcl-2: B-cell lymphoma-2; XBP-1: X-box binding protein I; Bim: Bcl-2 interacting mediator of cell death; BSYZ-F: Bushen Yizhi Formula.

In terms of the relationship between ERS and AD, IRE1α has attracted the most attention in ongoing research (Montibeller and de Belleroche, 2018; Sadleir *et al.*, 2018). Since IRE1α dissociates from GRP78, conformational changes rapidly activate its kinase activity, and autophosphorylation activates its endoribonuclease activity (Arag *et al.*, 2009; Ali *et al.*, 2011). Activated IRE1α converts the precursor mRNA of XBP-1 into mature mRNA, and then transmits the UPR signal downstream in this manner. In our study, to further explore the specific mechanism of Bushen Yizhi Formula in the treatment of AD, we also probed changes in the IRE1α signaling pathway. Our results demonstrate that Aβ increased the expression of p-IRE1α in the cell lines and rat brain neurons. In addition, we also found that the expression levels of p-JNK, Bax, XBP-1, and Bim was increased by Aβ treatment, while the expression of Bcl-2 was decreased. It is worth noting that IRE1α controls cellular fate determination through mitotic kinase JNK during ERS (Hetz and Glimcher, 2009; Merksamer and Papa, 2010).

Furthermore, our test results found that the Bushen Yizhi Formula could partially reverse the regulatory effects of Aβ on p-IRE1α, p-JNK, Bax, Bcl-2, XBP-1, and Bim. However, ASK1 expression did not change significantly. During ERS, the activation of IRE1 could recruit tumor necrosis factor, while IRE1-TRAF2 could further recruit apoptotic signal regulating kinase 1 to form the IRE1-TRAF2-ASK1 complex, which activates the apoptosis caused by JNK (Madeo and Kroemer, 2009). Our test results showed that neither Aβ stimulation nor Bushen Yizhi Formula could cause changes in ASK1 expression. As for the specific mechanism involved, it needs to be further explored. This may be an important reason why the kidney-tonifying prescription cannot completely reverse the effect of Aβ on AD.

In conclusion, our experimental results show that the Bushen Yizhi Formula can affect the expressions of p-JNK, Bax, Bcl-2, XBP-1, and Bim by regulating the phosphorylation of IRE1α. Notably, IRE1α, JNK, Bax, Bcl-2, XBP-1, and Bim are all ERS-related proteins. Our results suggest that the Bushen Yizhi Formula can affect ERS through the IRE1α signaling pathway to achieve its therapeutic effect on AD. These findings provide new regulatory mechanisms and evidence for the Bushen Yizhi Formula in the treatment of AD. Traditional Chinese Medicine has the feature of "multiple active ingredients, multiple targets", so more analyses on the target or active ingredient of Bushen Yizhi Formula for AD treatment are required in the future.

Funding Statement: This work was supported by the National Natural Science Foundation of China [81904266, 82004309].

Author Contributions: The authors confirm contribution to the paper as follows: study conception and design: Xiru Xu,

Yuan Fang, Biao Zhang; data collection: Yuan Fang, Shichao Teng and interpretation of results: Xiang Wu, Jing Zhang, Xiaoqun Gu, Meixia Ma; draft manuscript preparation: Xiru Xu, Yuan Fang, Biao Zhang. All authors reviewed the results and approved the final version of the manuscript.

Availability of Data and Materials: The analyzed data sets generated during the study are available from the corresponding author upon reasonable request.

Ethics Approval: All animal experiments were conducted in accordance with the guidelines of the China Council on Animal Care and Use. All experiments involving animals were conducted at the Zhejiang Laboratory Animal Center and approved in advance by the Institutional Animal Care and Use Committee of Zhejiang Laboratory Animal Center (Approval No. ZJCLA-IACUC-20040024).

Conflicts of Interest: The authors declare that they have no conflicts of interest to report regarding the present study.

References

Ali MM, Bagratuni T, Davenport EL, Nowak PR, Silva-Santisteban MC et al. (2011). Structure of the IRE1 autophosphorylation complex and implications for the unfolded protein response. *The EMBO Journal* **30**: 894–905. https://doi.org/10.1038/emboj.2011.18

Alzheimer's Association (2016). 2016 Alzheimer's disease facts and figures. *Alzheimer's & Dementia* **12**: 459–509. https://doi.org/10.1016/j.jalz.2016.03.001

Arag N, Van Anken T, Pincus E, Serafimova DIM, Korennykh AV, Rubio CA, Walter P (2009). Messenger RNA targeting to endoplasmic reticulum stress signalling sites. *Nature* **457**: 736–740. https://doi.org/10.1038/nature07641

Cai H, Luo Y, Yan X, Ding P, Huang Y et al. (2018). The mechanisms of Bushen-Yizhi formula as a therapeutic agent against Alzheimer's disease. *Scientific Reports* **8**: 3104. https://doi.org/10.1038/s41598-018-21468-w

Chen Y, Brandizzi F (2013). IRE1: ER stress sensor and cell fate executor. *Trends in Cell Biology* **23**: 547–555. https://doi.org/10.1016/j.tcb.2013.06.005

Davis AA, Leyns CEG, Holtzman DM (2018). Intercellular spread of protein aggregates in neurodegenerative disease. *Annual Review of Cell and Developmental Biology* **34**: 545–568. https://doi.org/10.1146/annurev-cellbio-100617-062636

Duran-Aniotz C, Cornejo VH, Espinoza S, Ardiles Á, Medinas O et al. (2017). IRE1 signaling exacerbates Alzheimer's disease pathogenesis. *Acta Neuropathologica* **134**: 489–506. https://doi.org/10.1007/s00401-017-1694-x

Endres K, Reinhardt S (2013). ER-stress in Alzheimer's disease: Turning the scale? *American Journal of Neurodegenerative Disease* **2**: 247–265.

Feldman HC, Vidadala VN, Potter ZE, Papa FR, Backes BJ, Maly DJ (2019). Development of a chemical toolset for studying the paralog-specific function of IRE1. *ACS Chemical Biology* **14**: 2595–2605. https://doi.org/10.1021/acschembio.9b00482

Fu XL, Gao DS (2014). Endoplasmic reticulum proteins quality control and the unfolded protein response: The regulative mechanism of organisms against stress injuries. *Biofactors* **40**: 569–585. https://doi.org/10.1002/biof.1194

Gardner BM, Pincus D, Gotthardt K, Gallagher CM, Walter P (2013). Endoplasmic reticulum stress sensing in the unfolded protein response. *Cold Spring Harbor Perspectives in Biology* **5**: a013169. https://doi.org/10.1101/cshperspect.a013169

Hashimoto S, Saido TC (2018). Critical review: Involvement of endoplasmic reticulum stress in the aetiology of Alzheimer's disease. *Open Biology* **8**: 180024. https://doi.org/10.1098/rsob.180024

Hedskog L, Pinho CM, Filadi R, RNNB CK, Hertwig A et al. (2013). Modulation of the endoplasmic reticulum-mitochondria interface in Alzheimer's disease and related models. *Proceedings of the National Academy of Sciences of the United States of America* **110**: 7916–7921. https://doi.org/10.1073/pnas.1300677110

Hetz C, Glimcher LH (2009). Fine-tuning of the unfolded protein response: Assembling the IRE1alpha interactome. *Molecular Cell* **35**: 551–561. https://doi.org/10.1016/j.molcel.2009.08.021

Hillary RF, Fitzgerald U (2018). A lifetime of stress: ATF6 in development and homeostasis. *Journal of Biomedical Science* **25**: 48. https://doi.org/10.1186/s12929-018-0453-1

Hou XQ, Wu DW, Zhang CX, Yan R, Yang C et al. (2014). Bushen-Yizhi formula ameliorates cognition deficits and attenuates oxidative stress-related neuronal apoptosis in scopolamine-induced senescence in mice. *International Journal of Molecular Medicine* **34**: 429–439. https://doi.org/10.3892/ijmm.2014.1801

Ibrahim IM, Abdelmalek DH, Elfiky AA (2019). GRP78: A cell's response to stress. *Life Sciences* **226**: 156–163. https://doi.org/10.1016/j.lfs.2019.04.022

Jung KJ, Min KJ, Bae JH, Kwon TK (2015). Carnosic acid sensitized TRAIL-mediated apoptosis through down-regulation of c-FLIP and Bcl-2 expression at the post translational levels and CHOP-dependent up-regulation of DR5, Bim, and PUMA expression in human carcinoma caki cells. *Oncotarget* **6**: 1556–1568. https://doi.org/10.18632/oncotarget.2727

Li K, Wei Q, Liu FF, Hu F, Xie AJ, Zhu LQ, Liu D (2018). Synaptic dysfunction in Alzheimer's disease: Aβ, tau, and epigenetic alterations. *Molecular Neurobiology* **55**: 3021–3032. https://doi.org/10.1007/s12035-017-0533-3

Liu XH, Ning FB, Zhao DP, Chang YY, Wu HM, Zhang WH, Yu AL (2021). Role of miR-211 in a PC12 cell model of Alzheimer's disease via regulation of neurogenin 2. *Experimental Physiology* **106**: 1061–1071. https://doi.org/10.1113/EP088953

Logue SE, Cleary P, Saveljeva S, Samali A (2013). New directions in ER stress-induced cell death. *Apoptosis* **18**: 537–546. https://doi.org/10.1007/s10495-013-0818-6

Madeo F, Kroemer G (2009). Intricate links between ER stress and apoptosis. *Molecular Cell* **33**: 669–670. https://doi.org/10.1016/j.molcel.2009.03.002

Mckhann GM, Knopman DS, Chertkow H, Hyman BT, Jack CR Jr et al. (2011). The diagnosis of dementia due to Alzheimer's disease: Recommendations from the National Institute on Aging-Alzheimer's Association workgroups on diagnostic guidelines for Alzheimer's disease. *Alzheimer's & Dementia* **7**: 263–269. https://doi.org/10.1016/j.jalz.2011.03.005

Merksamer PI, Papa FR (2010). The UPR and cell fate at a glance. *Journal of Cell Science* **123**: 1003–1006. https://doi.org/10.1242/jcs.035832

Montibeller L, de Belleroche J (2018). Amyotrophic lateral sclerosis (ALS) and Alzheimer's disease (AD) are characterised by differential activation of ER stress pathways: Focus on UPR

target genes. *Cell Stress Chaperones* **23**: 897–912. https://doi.org/10.1007/s12192-018-0897-y

Qi Z, Chen L (2019). Endoplasmic reticulum stress and autophagy. *Advances in Experimental Medicine and Biology* **1206**: 167–177. https://doi.org/10.1007/978-981-15-0602-4

Sadleir KR, Popovic J, Vassar R (2018). ER stress is not elevated in the 5XFAD mouse model of Alzheimer's disease. *Journal of Biological Chemistry* **293**: 18434–18443. https://doi.org/10.1074/jbc.RA118.005769

Shi J, Sabbagh MN, Vellas B (2020). Alzheimer's disease beyond amyloid: Strategies for future therapeutic interventions. *British Medical Journal* **371**: m3684. https://doi.org/10.1136/bmj.m3684

Song S, Tan J, Miao Y, Zhang Q (2018). Crosstalk of ER stress-mediated autophagy and ER-phagy: Involvement of UPR and the core autophagy machinery. *Journal of Cellular Physiology* **233**: 3867–3874. https://doi.org/10.1002/jcp.26137

Sweeney MD, Sagare AP, Zlokovic BV (2018). Blood-brain barrier breakdown in Alzheimer disease and other neurodegenerative disorders. *Nature Reviews Neurology* **14**: 133–150. https://doi.org/10.1038/nrneurol.2017.188

Tanzi RE (2012). The genetics of Alzheimer disease. *Cold Spring Harbor Perspectives in Medicine* **2**: a006296. https://doi.org/10.1101/cshperspect.a006296

Tiwari S, Atluri V, Kaushik A, Yndart A, Nair M (2019). Alzheimer's disease: Pathogenesis, diagnostics, and therapeutics. *International Journal of Nanomedicine* **14**: 5541–5554. https://doi.org/10.2147/IJN.S200490

Tracy TE, Gan L (2018). Tau-mediated synaptic and neuronal dysfunction in neurodegenerative disease. *Current Opinion in Neurobiology* **51**: 134–138. https://doi.org/10.1016/j.conb.2018.04.027

Wong KH, Riaz MK, Xie Y, Zhang X, Liu Q, Chen H, Bian Z, Chen X, Lu A, Yang Z (2019). Review of current strategies for delivering Alzheimer's disease drugs across the blood-brain barrier. *International Journal of Molecular Sciences* **20**: 381. https://doi.org/10.3390/ijms20020381

Yasmeen N, Datta M, Kumar V, Alshehri FS, Almalki AH, Haque S (2022). Deciphering the link between ER(UPR) signaling and MicroRNA in pathogenesis of Alzheimer's disease. *Frontiers in Aging Neuroscience* **14**: 880167. https://doi.org/10.3389/fnagi.2022.880167

Zhang C (2017). Roles of Grp78 in female mammalian reproduction. *Advances in Anatomy, Embryology and Cell Biology* **222**: 129–155. https://doi.org/10.1007/978-3-319-51409-3

Zhang SJ, Luo D, Li L, Tan RR, Xu QQ et al. (2017a). Ethyl acetate extract components of Bushen-Yizhi formula provides neuroprotection against scopolamine-induced cognitive impairment. *Scientific Reports* **7**: 9824. https://doi.org/10.1038/s41598-017-10437-4

Zhang SJ, Xu TT, Li L, Xu YM, Qu ZL et al. (2017b). Bushen-Yizhi formula ameliorates cognitive dysfunction through SIRT1/ER stress pathway in SAMP8 mice. *Oncotarget* **8**: 49338–49350. https://doi.org/10.18632/oncotarget.17638

Supplementary Materials

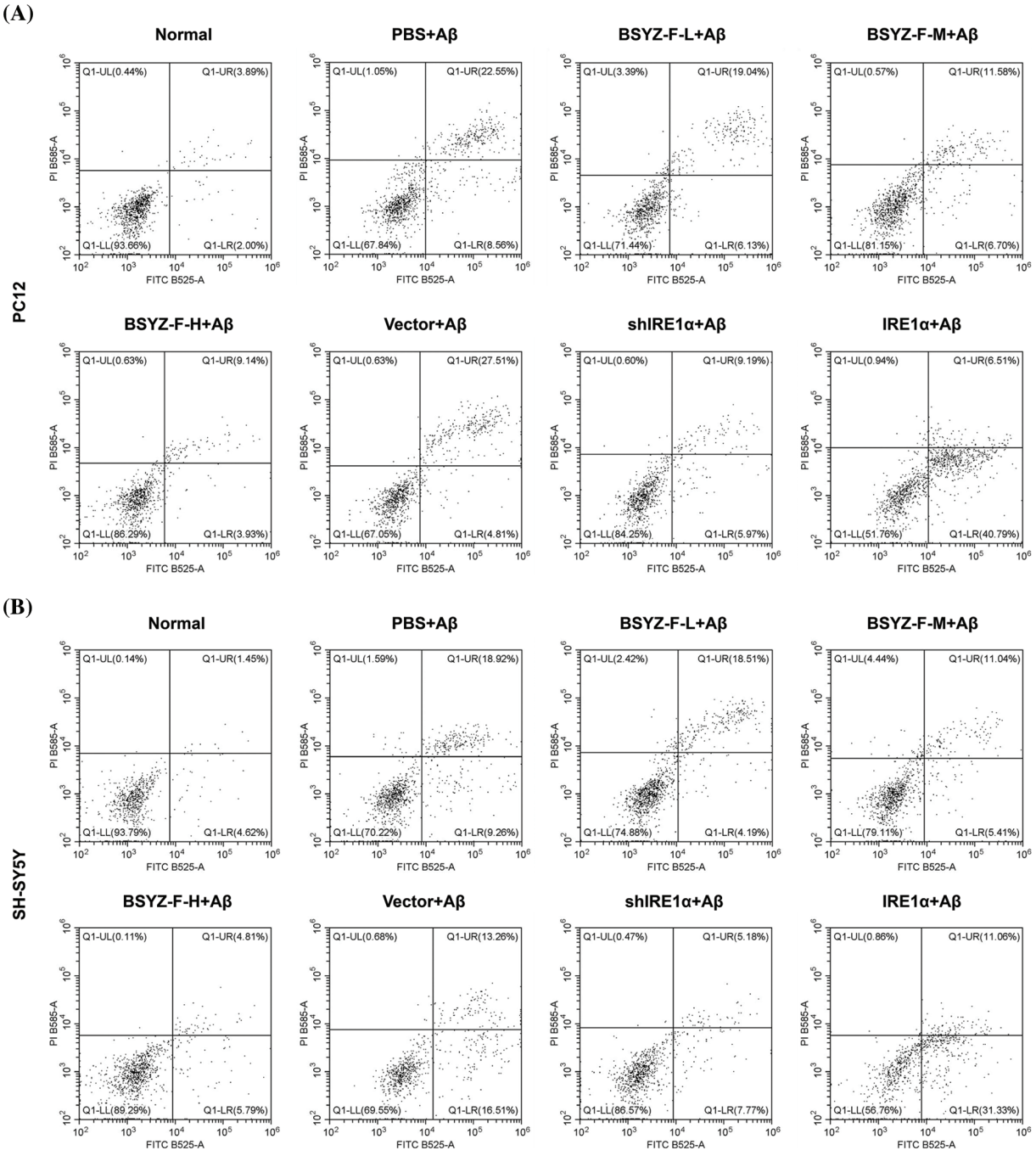

SUPPLEMENTARY FIGURE 1. The apoptosis profile of PC12 and SH-SY5Y cells was measured by flow cytometry.

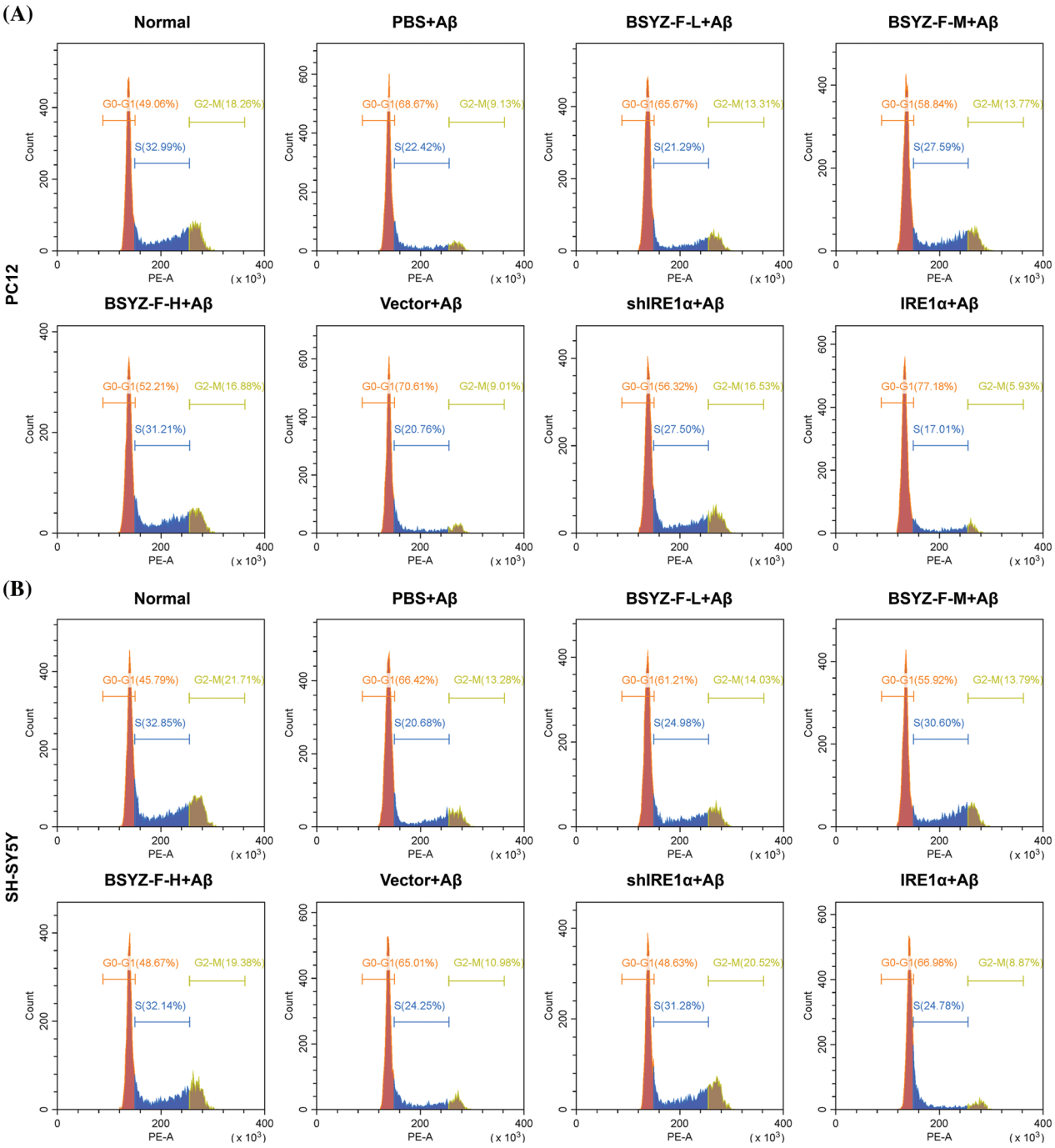

SUPPLEMENTARY FIGURE 2. The cell cycle in PC12 and SH-SY5Y cells was assayed by flow cytometry.